



INVESTIGATING CURRENT DENSITY DEPENDENCE OF OXIDE TRAP CHARGING IN n-MOSFETS DURING SUBSTRATE ELECTRONS INJECTION: A GENETIC ALGORITHM APPROACH

Idrees S. AL-Kofahi

Electrical Engineering Department, Faculty of Engineering, Al Jouf University, Sakaka, Saudi Arabia
eskofhee@ju.edu.sa

Received 11-02-2013, accepted 20-02-2013, online 21-02-2013

Abstract In this paper the reliability of n-channel MOSFETs using the Substrate Hot Electron (SHE) technique is considered. The technologically important low field case ($E_{ox} < 2$ MV/cm) for a current densities range from 0.02 to 2 mA/cm² and injected charge densities up to 10 C/cm² is considered here in some detail. We confirm previous results reported by ourselves and others that there is a dependence of oxide degradation upon the current density during SHE injection. The dynamic trapping and detrapping of previously trapped electrons are taken into account to explain these results. A power law model is presented which accounts for the detrapping phenomenon. Genetic algorithm is used to extract the parameters of the model.

Keywords: Substrate Electron Injection, MOSFET Reliability, Electron Traps, Genetic Algorithm

I. INTRODUCTION

The success of CMOS technologies strongly relies on the excellent insulating properties of gate silicon dioxides and their near-perfect interface with silicon. As the device size reduces, the electrical field within the device increases. This causes damage to the oxide [1–6] and its interface with silicon [4–7], which has become a major reliability concern for the CMOS technology.

Defects in SiO₂ or at its interface with Si can have a number of adverse effects on devices such as an increase in gate leakage current [8-11], and oxide breakdown [9-10]. Three types of defects have been identified: interface states [5], electron traps [5,12-13] and hole traps [14-16] generation.

One main source for device instabilities is the electron trapping and trap generation in the gate dielectric [1-6, 12, 17-18]. The electron traps affect devices through capturing electrons and building up space charges, which shift parameters such as threshold voltage and transconductance [5,6]. For the thin gate oxide used in the current and future generations of CMOS processes, electron trap generation causes two additional reliability problems. First, electron traps can assist electrons passing through the dielectric and this stress-induced leakage current (SILC) can considerably reduce the nonvolatile memory retention time [8–11]. Second, the build-up of electron traps triggers the dielectric breakdown [1,2].

Instabilities can be induced in the bulk of SiO₂ under a number of stress conditions, such as hot carrier injection [5-7], Fowler-Nordheim injection [12,13], irradiation [19] and bias temperature stress [17,20].

An effective procedure for studying electrically active bulk defects involves the uniform injection of a single carrier type across the Si/SiO₂ while monitoring the shift in the threshold voltage (ΔV_{th}) or flatband voltage (ΔV_{fb}) which is a measure of the fraction of these injected carriers that get trapped. Such an experiment emulates hot channel carrier injection and trapping, to a degree, but in a much more controlled fashion.

Electrons can be injected into the oxide either uniformly [2,6,21] or non-uniformly [4,5]. In this study, uniform electron injection along the channel is used to avoid uncertainties in the lateral distribution of trapped electrons and created defects. Substrate hot electron injection is a technique which may be used on transistor to inject electron to the oxide at low electric field. The technique has the advantage that the injection of electrons is uniform and the oxide field and injection current density can be varied independently [21]. Using this technique therefore, it becomes possible to distinguish between the charge trapping dependence on oxide field and on the injection current density.

II. DEVICES AND EXPERIMENTS

II.1 Devices

The devices used in this study are n-MOSFETs fabricated by a 0.5 μ m CMOS technology. The oxide was grown in dry O₂ to a thickness of 15 nm. The n-MOSFETs were surface channel devices, with n⁺ poly-Si gate. The p-well was heavily doped to a level of 3 \times 10¹⁶ cm⁻³ and no threshold voltage adjustment implantation was carried out. The channel length is in the range of 5 to 50 μ m and the channel width is 100 μ m.

II.2 Experiments

To simplify the experimental condition, electrons are uniformly injected into the oxide by using the substrate hot electron injection technique [21]. Figure 1 shows the schematic illustration of the SHE measurement setup. Hot electrons are supplied by forward biasing the underlying p-well/n-substrate junction. Electrons reach the space charge layer are heated and accelerated towards the Si/SiO₂ interface by the p-well bias (V_w). With the source and drain grounded, the majority of these electrons are collected by the source and drain, while some

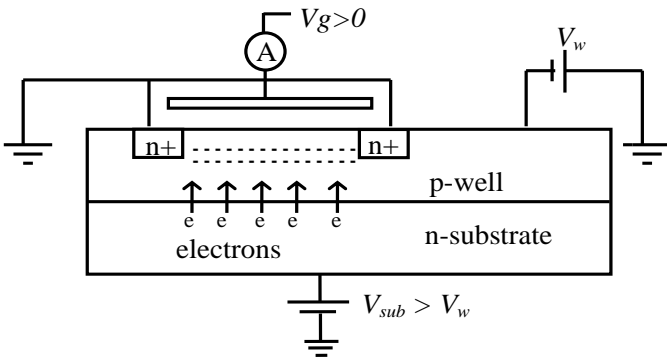


Figure 1: Schematic representation of substrate hot electron injection.

of the most energetic ones can be injected into the oxide. In inversion, the silicon and (positive) oxide field can be independently controlled by adjusting the p-well bias and the gate bias (V_g), respectively [16,21]. To keep energy of the injected electrons constant, the injection current density was controlled by automatically adjusting the substrate voltage while the well bias was kept fixed. During the entire SHE, the oxide field and injection current density were fixed. The total injected electron density (N_{inj}) was determined from the gate current. During the stress, the electron injection is periodically interrupted to monitor the build-up of trapped electrons and interface states. The interface states were measured by using the standard two-level charge-pumping technique [23]. The density of trapped electrons was measured from the shift of the transfer characteristics in the subthreshold region [21]. The contribution of the generated interface states to this shift was generally negligible. The centroid of trapped charges is not known under our testing conditions. In such circumstances, it has been commonly assumed that the centroid is at the Si/SiO₂ interface and the equivalent charge density is referred to as the effective charge density [22,24]. In this paper, we follow early works [22,24] and present the results in terms of this effective charge density, N_e .

III. AVAILABLE MODELS

The trapped electron in the oxide can be measured from the shift in the threshold or flatband voltage versus the total dose, fluence, of injected carriers. Different models were proposed to explain the buildup of trapped electrons with injected charges. The trapped electrons in the oxide have generally been modeled using a first order trapping model.

III.1 First Order Trapping Model

The effect of charge trapping can be understood by characterizing the defects in term of their capture cross section, σ and as grown (native) traps density, N_o . To determine σ and N_o , first order trapping kinetics have been used to model electron trapping in the gate insulators of MOSFETs. In this model, it is assumed that a trap can be occupied by only one electron, that is, its cross section and density are constant, and the depopulation rate is insignificant compared to the population rate. From first order trapping kinetics, it can be shown that for a single type

of trap, the measured filled traps (ΔN_e) as a function of N_{inj} , can be expressed as [25] :

$$\Delta N_e = N_o \left[1 - e^{-N_{inj} \sigma} \right] \quad (1)$$

$$N_{inj} = \frac{1}{q} \int_0^t J_{inj} dt \quad (2)$$

where, N_o and σ are as grown trap density and capture cross section, respectively and J_{inj} is the injection current density at the Si/SiO₂.

Equation (1) accommodates the filling of only a single type of trap, and requires that the total number of such traps (filled plus unfilled) be a constant. Based on such model, traps of capture cross sections ranging from 10⁻¹³ - 10⁻²⁰ cm² have been proposed in intrinsic state of the art insulators. If more than one type of trap is present over the range of data acquired, then the total measured charged traps would be the sum of two or more equations of the type given in equation (1) and can be expressed as:

$$\Delta N_e = \sum_{i=1}^k N_{o,i} \left[1 - e^{-N_{inj} \sigma_i} \right] \quad (3)$$

III.2 Charged Bulk Defect Generation:

Trap filling under low electric field has been studied and modeled [12,13,17,18]. However, very little has been done to model oxide trap generation. Electron trap generation at high electric field has been modeled using a linear term [26]. In a different study, a power law has been used to describe interface states [27] and bulk charges [28,29] build up during channel hot carrier injection. Defect generation in n-channel insulated gate field effect transistor using an optically assisted hot electron injection technique was proposed by Kim *et.al.*[30]. They employed a power law to model the bulk defect generation (N_G) resulting from uniform substrate hot electron injection and they have chosen to express this model in terms of N_{inj} , to be consistent with the first order model, as:

$$N_G = \eta N_{inj}^\beta \quad (4)$$

where: η and β are the parameters of the model.

In cases were there might be both the filling of existing bulk traps and the generation of new charged defects, they suggested the use of a combination of the two models by simply adding equation (1) and equation (4) to give the general equation:

$$\Delta N_e = \eta N_{inj}^\beta + N_o \left[1 - e^{-N_{inj} \sigma} \right] \quad (5)$$

This assumes that the two mechanism are independent of each other.

IV. APPLICATION OF THE GENETIC ALGORITHM METHOD

Genetic algorithm (GA) is a search procedure inspired by population genetics. It has excellent search capabilities for finding a good and global solution to a problem without a prior information about the nature of the problem [31,32]. Computationally, the implementation of a typical GA is quite simple and consists of five basic steps. These include (i) initialization of a chromosome population, (ii) evaluation of

the population, (iii) selection of the parent chromosome for breeding and mating, (iv) crossover and mutation, and finally (v) replacing parents with their offspring.

A chromosome consists of a set of genes $\{g_1, g_2, g_3, \dots, g_n\}$, which represents the whole potential solution to the desired equation. For three fitting parameters $\{N_o, \alpha, \sigma\}$ the chromosome can be written as:

$$chro = \{N_o, \alpha, \sigma\} \quad (6)$$

In the initialization step, the first generation of chromosomes is created randomly with a fixed population size. The values of the genes are also determined randomly between fixed low and high limits. Once the initial chromosome population is created, the next step is to evaluate and rank the chromosome, from smallest to largest, using a fitness function, which is the error square given by:

$$e = \sum_{k=1}^n \sum_{l=1}^m \left[N_e(J_{inj_k}) - \hat{N}_e(J_{inj_k}) \right]^2 \quad (7)$$

where m is the number of experimental data at a specific injection current density (J_{inj}) and n is the number of injection current densities. The first term on the right-hand side of equation (7) is the experimentally determined electron traps and the second term is the theoretically expected ones. The third step involves the selection of the parent chromosomes from the current population for breeding, where the unacceptable chromosomes are discarded. The fourth step is to pair the remaining chromosomes of survivals for mating in a crossover operation described by:

$$child_1 : \begin{cases} N_o = r N_{o1} + (1-r) N_{o2} \\ \alpha = r \alpha_1 + (1-r) \alpha_2 \\ \sigma = r \sigma_1 + (1-r) \sigma_2 \end{cases} \quad (8)$$

$$child_2 : \begin{cases} N_o = (1-r) N_{o1} + r N_{o2} \\ \alpha = (1-r) \alpha_1 + r \alpha_2 \\ \sigma = (1-r) \sigma_1 + r \sigma_2 \end{cases} \quad (9)$$

where $\{N_{o1}, \alpha_1, \sigma_1\}$ and $\{N_{o2}, \alpha_2, \sigma_2\}$ are two survival chromosomes, and $r \in (0, 1)$ is a random number called a weighted average operator. To prevent the premature convergence to local optima, a mutation operation can be used, which can be described by:

$$N_o = N_o + (r_1 - 0.5)(2N_{o_{max}} - N_o) \quad (10)$$

$$\alpha = \alpha + (r_2 - 0.5)(2\alpha_{max} - \alpha) \quad (11)$$

$$\sigma = \sigma + (r_3 - 0.5)(2\sigma_{max} - \sigma) \quad (12)$$

where $N_{o_{max}}$, α_{max} and σ_{max} are the maximum allowable changes of N_o , α and σ , respectively and r_1, r_2 and $r_3 \in (0, 1)$ are random numbers with low probability. After mutation, the survived chromosomes and offsprings are evaluated and ranked, and the genetic operators are repeated until the termination condition is satisfied. The chromosome with the highest fitness value, which is the lowest error squared, is adapted as a final solution to the problem.

In this paper the genetic algorithm method is used to analyze electron traps measured during SHE injection at different injection current densities. Details of the used

sample and experiment is shown in devices and experiments section.

V. RESULTS AND DISCUSSION

Figure 2 shows variation of trapped charges as a function of injected electrons measured at seven injection current densities. The data points represent the actual experimental data points. An increase in the trapped charges with increasing J_{inj} and/or N_{inj} is obvious which supports previously reported results [21, 30]. To explain these results genetic algorithm is used to fit these data to the available

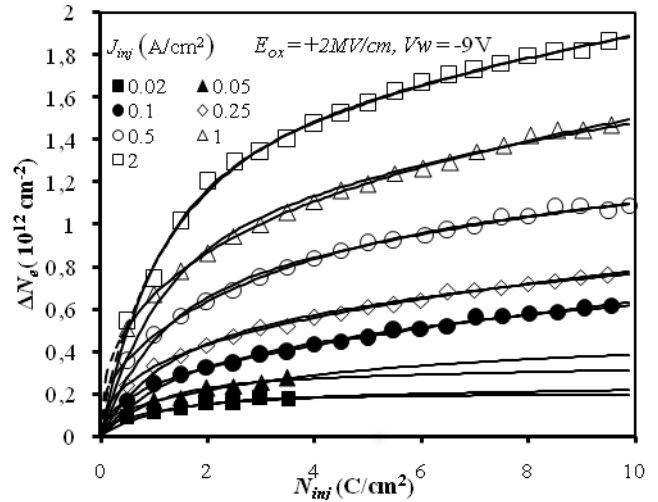


Figure 2: Trapped electrons during SHE under different J_{inj} . Measured (symbols), calculated using equation (3) (solid lines) and using equation (5) (dashed lines)

models presented by equation (1), equation (3), equation (4) and equation (5).

The generation model (equation 4) and a single first order trapping model (equation 1) were unable to explain the dependence of the obtained results on N_{inj} and J_{inj} (not shown), while the result of fitting the data to equation (3) and equation (5) are show in figure 2. In the figure, the dashed lines show the result of fitting the obtained data to the first order trapping model with two capture cross section (equation (3) with $k=2$), while the solid lines show the result of fitting the obtained data to equation (5). The resulting fitting parameters are given in table 1 and table 2, respectively. It is clear from the tables that the obtained fitting parameters are different for different injection current density and the two models could explain the dependence of trapped charges on N_{inj} , but the those models fail to explain the dependence of trapped charges injection current density. Therefore, another model should be used to explain the obtained result.

Schwerin and Heyns [21] argued that dynamic trapping-detraping model [25] could not explain the dependence of trapped charges on J_{inj} . Their conclusion was based on applying electric field after SHE without electron injection. They found that the oxide electric field has no effect on the trapped electrons. It is worth mentioning that their experimental condition post SHE ($J_{inj}=0$) was different from that during the injection. During the SHE energetic electrons are injected to the oxide and passed through it. The injected electrons may trigger trapped electrons and cause detrapping of the previously trapped electrons. To study the effect of electrons injection on

the trapped electron, two experiments were carried out. In the first experiment, three devices were stressed by SHE under

Table 1: Fitting parameters of two first-order trapping model (equation 3)

J_{inj} (mA cm ⁻²)	N_1 (10 ¹² cm ⁻²)	N_2 (10 ¹² cm ⁻²)	σ_1 (10 ⁻¹⁹ m ²)	σ_2 (10 ⁻¹⁹ cm ²)
0.02	0.14607	0.04534	0.61820	9.94142
0.05	0.28934	0.09260	0.27763	5.25003
0.1	0.63096	0.18955	0.11818	2.41411
0.25	0.67162	0.26577	0.14117	2.53223
0.5	0.86171	0.31986	0.22601	3.31330
1	1.19158	0.53516	0.16141	2.84491
2	1.23268	0.98972	0.13023	1.08778

Table 2: Fitting parameters of trapping and generation model (equation 5)

J_{inj} (mA cm ⁻²)	N_o (10 ¹² cm ⁻²)	σ (10 ⁻¹⁹ cm ²)	η (10 ⁻²)	β
0.02	0.12907	0.63799	1.77074	0.10000
0.05	0.18545	0.24773	1.04833	0.24701
0.1	0.06416	1.94839	0.20523	0.48860
0.25	0.05804	0.95426	1.07983	0.39647
0.5	0.42218	0.31122	4.14064	0.28460
1	0.12469	0.57258	5.33415	0.35282
2	0.87802	0.79834	1.41411	0.50172

+2MV/cm and $J_{inj}=5 \times 10^{-4} \text{ A/cm}^2$ followed by low injection current density period. Figure 3 (Symbol 'Δ') shows the trapped electrons during the $J_{inj}=5 \times 10^{-4} \text{ A/cm}^2$ period. After injecting 3 C/cm², in one device, J_{inj} was reduced to zero (symbol '•'), while for the other two devices J_{inj} was reduced to $2 \times 10^{-5} \text{ A/cm}^2$ (symbol '□') for one of them and the other to $5 \times 10^{-5} \text{ A/cm}^2$ (symbol 'o'). As shown in figure 3, negligible change in the trapped electrons was observed when electrons were not injected in support of previously reported results [21]. However, when electrons were injected under low injection current density ($2 \times 10^{-5} \text{ A cm}^{-2}$ and $5 \times 10^{-5} \text{ A cm}^{-2}$), a decreasing in the trapped electrons rather than increasing was observed. This reduction in the trapped electrons could be explained by the larger detrapping rate compared to the trapping rate under low J_{inj} . To support this conclusion, another experiment was carried out. In this experiment, between every two subsequent characterization measurements, electrons were injected at $J_{inj}=5 \times 10^{-4} \text{ A/cm}^2$ for 0.45 C/cm² and then J_{inj} was reduced to $5 \times 10^{-5} \text{ A/cm}^2$ for another 0.05 C/cm². The trapped electrons are shown in figure 4 (symbol '•'). On the same figure trapped electrons in a device subjected to $J_{inj}=5 \times 10^{-4} \text{ A/cm}^2$ for the whole 0.5 C/cm² is shown by symbol 'Δ'.

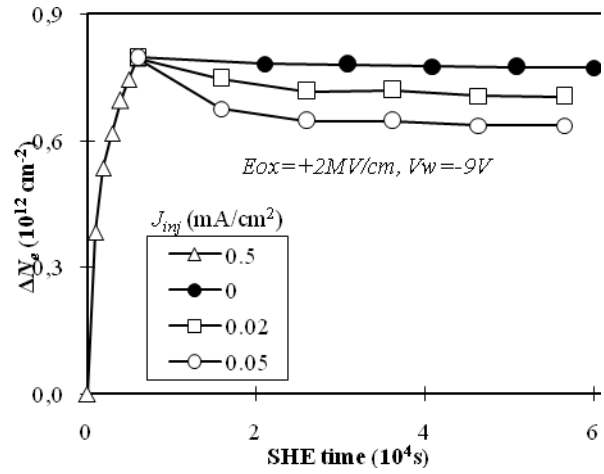


Figure 3: The effect of energetic electron injection on electron detrapping during SHE. After injecting 3C/cm² at $J_{inj}=5 \times 10^{-4} \text{ A/cm}^2$ (Symbol 'Δ'), J_{inj} was changed to zero (symbol '•'), to $J_{inj}=2 \times 10^{-5} \text{ A/cm}^2$ (symbol '□') and to $J_{inj}=5 \times 10^{-5} \text{ A/cm}^2$ (symbol 'o').

If electrons detrapping occurs during the injection, then it is expected that for longer injection time more electrons are detrapping. As a result, trapped electrons at low J_{inj} should be less than that at high J_{inj} , which can be seen clearly in figure 4.

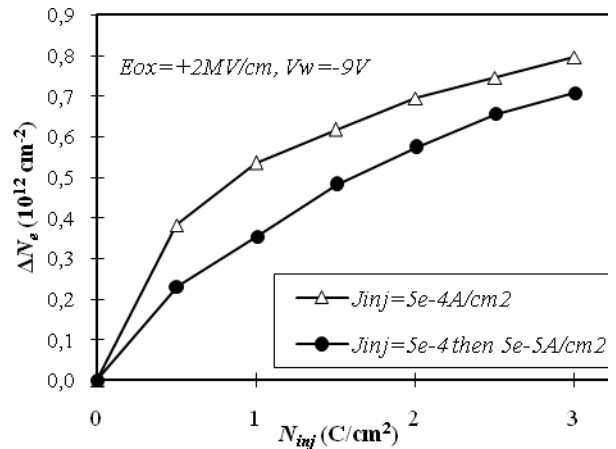


Figure 4: Trapped electrons at $J_{inj}=5 \times 10^{-4} \text{ A/cm}^2$ (Δ symbol) and that obtained by first injected at $J_{inj}=5 \times 10^{-4} \text{ A/cm}^2$ for 0.45 C/cm² followed by $J_{inj}=5 \times 10^{-5} \text{ A/cm}^2$ for another 0.05 C/cm² (• symbol).

The trapped electrons dependence on injection current density suggest that the first order trapping model with single capture cross section [31] should be modified to include the detrapping of previously trapped charges during injection in to account. If we assume that the detrapping is a power function of time, then the first order trapping model can be rewritten as

$$\Delta N_e(J_{inj}) = N_o \cdot t^\alpha \left[1 - e^{-N_{inj}\sigma} \right] \quad (13)$$

where: N_o and σ are as grown trap density and capture cross section, respectively, α is the detrapping rate of previously trapped electrons and the injection time is given by:

$$t = \frac{qN_{inj}}{J_{inj}} \quad (14)$$

By applying the above model to the experimental data, figure 5 is obtained. The solid lines in figure 5 show fitting the obtained data, using a genetic algorithm, to equation (13). The extracted parameters are: $N_o=1.07 \times 10^{14} \text{ cm}^{-2}$, $\sigma=1.64 \times 10^{-20} \text{ cm}^2$ and $\alpha=-0.422$. As clearly shown in the figure, a good agreement between experimental data and the proposed model is obtained, with minimum fitting parameters. The figure shows detrapping of previously trapped electrons is significant at low J_{inj} and a dynamic balance between trapping and detrapping is reached which explains the saturation of trapped charges with N_{inj} for $J_{inj} \leq 0.1 \text{ mA/cm}^2$. However, for $J_{inj} > 0.1 \text{ mA/cm}^2$ electrons trapping dominates which explains the non saturation behavior of trapped electrons with N_{inj} .

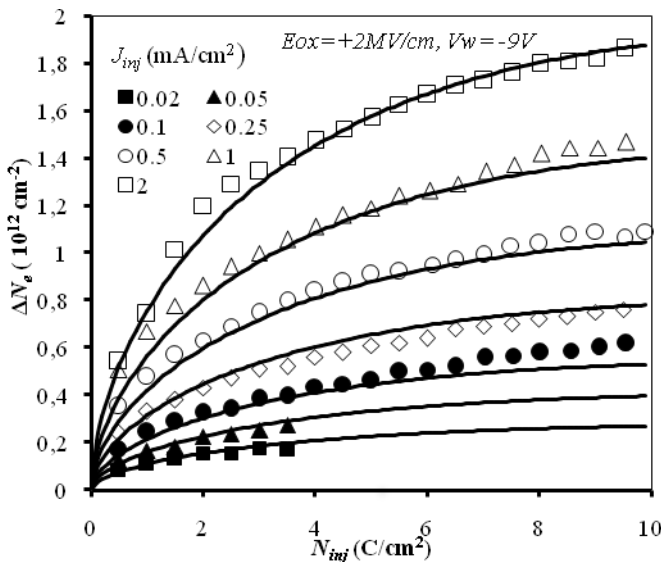


Figure 5: Trapped electrons during SHE under different J_{inj} . Measured (symbols) and calculated using equation (13) (solid lines)

VI. CONCLUSIONS

A genetic algorithm method coupled with the SHE experimental data is applied to explain the dependence of oxide bulk electrons trap charging on injection current density during SHE. The present results show that the detrapping of previously trapped electrons must be taken into account in order to explain this dependence. Based on trapping and detrapping a model has been proposed. The model shows good agreement with experimental results over the whole range considered. The fitting parameters of the model are determined by using genetic algorithm. The dependence of trapped electrons on J_{inj} is important for reliability prediction (using accelerated testing), emphasizing the importance of taking this dependence into consideration in device lifetime prediction.

References

- [1] B. Kaczer, R. Degraeve, N. Pagon, and G. Groeseneken, "The influence of elevated temperature on degradation and lifetime prediction of thin silicon-dioxide films", *IEEE Trans. Electron Devices*, **47**, 1514 (2000).
- [2] D. J. DiMaria, "Defect generation under substrate hot electron injection into ultrathin silicon dioxide layers", *J. Appl. Phys.*, **86**, 2100 (1999).
- [3] C. B. Park, Chang, "Investigation of the device instability feature caused by electron trapping in pentacene field effect transistors", *Appl. Phys. Lett.*, **100**, 063306, (2012).
- [4] J. Martín-Martínez, S. Gerardin, E. Amat, R. Rodríguez, M. Nafria, X. Aymerich, A. Paccagnella, and G. Ghidini, "Channel-hot-carrier degradation and bias temperature instabilities in CMOS inverters", *IEEE Trans. Electron Devices*, **56**, 2155 (2009)
- [5] R. Woltjer, A. Hamada, and E. Takeda, "Time-dependence of pMOSFET hot-carrier degradation measured and interpreted consistently over ten orders of magnitude", *IEEE Trans. Electron Devices*, **40**, 392 (1993).
- [6] G. Groeseneken, R. Bellens, G. Van den Bosch, and H. E. Maes, "Hot-carrier degradation in submicrometer MOSFETs: From uniform injection toward the real operating conditions", *Semicond. Sc. Technol.*, **10**, 1208 (1995).
- [7] A. Bravaix, D. Goguenheim, N. Revil, and E. Vincent, "Hot-carrier reliability study of second and first impact ionization degradation in 0.15- μm channel-length NMOSFETs", *Microelectron. Eng.*, **59**, 101 (2001).
- [8] D. Ielmini, A. S. Spinelli, M. A. Rigamonti and A. L. Lacaita "Modeling of SILC based on electron and hole tunneling—part I: transient effects", *IEEE Trans. Electron Devices*, **47**, 1258 (2000).
- [9] S. Bruyere, D. Roy, E. Robilliart, E. Vincent and G. Ghibaudo "Body effect-induced wear-out acceleration in ultra-thin oxides", *Microelectron. Reliab.*, **41**, 1031 (2001).
- [10] D. J. DiMaria and J. H. Stathis "Anode hole injection, defect generation, and breakdown in ultrathin silicon dioxide films", *J. Appl. Phys.*, **89**, 5015 (2001).
- [11] A. Scarpa, G. Tao, J. Dijkstra, and F. G. Kuper, "Tail bit implications in advanced 2 transistors-Flash memory device reliability," *Microelectron. Eng.*, **59**, 183 (2001).
- [12] W. D. Zhang, J. F. Zhang, M. Lalor, D. Burton, G. Groeseneken and R. Degraeve "Two Types of Neutral Electron Traps Generated in the Gate Silicon Dioxide", *IEEE Trans. Electron Devices*, **49**, 1868 (2002).
- [13] D. J. DiMaria, D. A. Buchanan, J. H. Stathis and R. E. Stahlbush "Interface states induced by the presence of trapped holes near the silicon-silicon-dioxide interface", *J. Appl. Phys.*, **77**, 2032 (1995).

- [14] J. F. Zhang, I. S. Al-Kofahi and G. Groeseneken, "Behavior of hot hole stressed SiO₂/Si interface at elevated temperature", *J. Appl. Phys.*, **83**, 843 (1998).
- [15] I. S. Al-Kofahi, J. F. Zhang and G. Groeseneken, "Continuing degradation of SiO₂/Si interface after hot hole stress", *J. Appl. Phys.*, **81**, 2686 (1997).
- [16] G. van den Bosch, G. Groeseneken, H. E. Maes, R. B. Klein and N. S. Saks "Oxide and interface degradation resulting from substrate hot-hole injection in metal-oxide-semiconductor field-effect transistors at 295 and 77 K," *J. Appl. Phys.*, **75**, 2073 (1994).
- [17] Wei-Liang Lin Jen-Chung Lou Yao-Jen Lee Tien-Sheng Chao, "Trapping/De-trapping Characteristics of Electrons and Holes Under Dynamic Nbti Stress on Hfo2 and Hfsion Gate Dielectrics", *Physical and Failure Analysis of Integrated Circuits, IPFA 2009. 16th IEEE International Symposium*, pp.122-125 (2009).
- [18] G. W. Karner, M. Sverdlov, V. T. Grasser, "A Rigorous Model for Trapping and De-trapping in Thin Gate Dielectrics", *Physical and Failure Analysis of Integrated Circuits, IPFA 2008. 15th International Symposium*, pp.1-6 (2008).
- [19] N. S. Saks, C. M. Dozier and D. B. Brown, "Time dependence of interface trap formation in MOSFETs following pulsed irradiation", *IEEE Trans. Nucl. Sc.*, **35**, 1168 (1988).
- [20] Y. Hiruta, H. Iwai, F. Matsuoka, K. Hama, K. Maeguchi and K. Kanzaki, "Interface state generation under long-term positive-bias temperature stress for a p⁺ poly gate MOS structure", *IEEE Trans. Electron Devices*, **36**, 1732 (1989).
- [21] A. v. Schwerin and M. M. Heyns, "Oxide field-dependence of bulk and interface trap generation in SiO₂ due to electron injection", in *Proc 7th Insulating Films on Semiconductors Conf.*, W. Eccleston and M. Uren, Eds., Bristol, U.K., pp. 263-266 (1991).
- [22] A. v. Schwerin, M. M. Heyns, and W. Weber, "Investigation on the oxide field-dependence of hole trapping and interface state generation in SiO₂ layers using homogeneous nonavalanche injection of holes," *J. Appl. Phys.*, **67**, 7595 (1990).
- [23] G. Groeseneken, H. E. Maes, N. Beltran, and R. F. De Keersmaecker, "A reliable approach to charge-pumping measurements in MOS transistors," *IEEE Trans. Electron Devices*, **ED-31**, 42 (1984).
- [24] D. J. DiMaria, "The properties of electron and hole traps in thermal silicon dioxide layers grown on silicon", *The Physics of SiO₂ and its interfaces*, S. T. Pantelides, Ed. New York:Pergamon, 1978, pp.160-178.
- [25] Y. Nissan-Cohen, J. Shappir and D. Frohman-Bentchkowsky, "Dynamic model of trapping-de-trapping in SiO₂", *J. Appl. Phys.*, **58**, 2252 (1985).
- [26] Y. Nissan-Cohen, J. Shappir and D. Frohman-Bentchkowsky, "Trap generation and occupation dynamics in SiO₂ under charge injection stress", *J. Appl. Phys.* **60**, 2024 (1986).
- [27] R. Bellens, E. de Schrijver, G. Van den Bosch, G. Groeseneken, P. Heremans and H. E. Maes, "On the hot-carrier-induced post-stress interface trap generation in n-channel MOS transistors", *IEEE Trans. Electron Dev.*, **41**, 419 (1994).
- [28] B. Doyle, M. Bourcier, J. C. Marchetaux and A. Boudou, "Interface State Creation and Charge Trapping in the Medium-to-High Gate Voltage Range ($V_d/2 \geq V_g$) During Hot-Carrier Stressing of n-MOS Transistors", *IEEE Trans. Electron Dev.* **37**, 744 (1990)
- [29] C. Hu, S. Tam, F. C. Hsu, P. K. Ko, T. Y. Chan and K. W. Terrill, "Hot-electron-induced MOSFET degradation---Model, monitor and improvement", *IEEE Trans. Electron Dev.* **ED-32**, 375 (1985).
- [30] H. S. Kim, C. K. Williams, and A. Reisman, "Low-field bulk defect generation during uniform carrier injection into the gate insulator of insulated gate field effect transistors at various temperatures", *Journal of Electronic Materials*, **27**, 908 (1998).
- [31] D. E. Goldberg, "Genetic Algorithms in Search, Optimization and Machine Learning", Addison-Wesley 1989.
- [32] A. Wright, "Genetic algorithms for real parameters optimization, in foundations of genetic algorithms", J. E. Rawlines, Ed. San Mateo CA: Morgan Kaufmann, 1991.